2 BACKGROUND AND FORMULATION OF DISTRIBUTED ADAPTIVE ARRAY CONCEPT

2.1 Introduction

This thesis investigates the advantage of combined beamforming vs. independent beamforming for distributed arrays. In addition the range increase relative to an omni antenna of adaptive and phased arrays in the presence of multipath and interferers is investigated. The purpose of this chapter is to set the background for the investigations to follow and to develop a mathematical formulation for the problem. The chapter starts by describing cellular network configurations with different frequency reuse patterns. This is followed by the concept of sectorization to improve the signal to noise ratio at the mobiles. Next, different array systems will be discussed followed by detail of the propagation channel models that will be used in the analysis.

This is followed by the definition of the distributed array system, consisting of arrays at alternate corners of a hexagonal cell. The narrowband (such as in TDMA and GSM systems) and wideband (such as in CDMA and UMTS systems) received signals at the arrays are defined, followed by independent and combined beamforming of these signals to produce an optimum receive signal to noise ratio (for the mobile signals) at the array outputs. Methods of estimating the beamforming weights are presented, followed by performance estimation methods of the array systems in a digital cellular network.

2.2 Cellular Network Definition

The concept of a cellular network is to reuse the same frequency in different cells. The radius (reuse distance) at which the same frequency can be reused is a function of the signal to interference ratio experienced by the mobiles or base stations. The interference from undesired mobiles received by base stations with omni-antennas is much higher than base stations with sectorized antennas. A reuse pattern of seven is typical for base stations with omni antennas, meaning that the same frequency is not used in the six cells surrounding a cell with a particular frequency. Sectorized antennas at the base station allows this reuse distance to be reduced, increasing the network number of mobiles or capacity that can be supported with sufficient signal to noise ratio. Sectorization and reuse distance are described next in more detail.

2.2.1 Sectorization

The number of mobiles that can be supported in each cell is a function of the signal to interference ratio that the mobiles experience. If the signal to noise ratio becomes lower than a certain threshold, the bit error rate will be too high to sustain the call and the call will be dropped or terminated. In order to reduce the interference, sectorization is used in the network. A network has typically three sectors (called tri-sectored in cellular networks). A tri-sectored base station will have three antennas, each with a 3dB beamwidth of 120° and with the boresight directions 120° apart. With sectorization, the reused distance can be reduced and a reuse of three is possible (this will be discussed in section 2.2.2)

A further decrease in interference to mobiles can be achieved with multibeam antennas in each sector with adaptive arrays. Adaptive arrays will tend to maximize the signal to interference ratios of a mobile by steering "nulls" in the directions of the interfering mobiles. The phased array, multibeam and adaptive arrays will be discussed in section 2.3) Adaptive arrays allows a reuse of one as well as same cell co-channel users [22].

2.2.2 Networks with Different Reuse Patterns

The geometry for a network with a frequency reuse pattern of three is shown in Figure 1 [49,50]. The first, second and third tier of interferers are also shown. A reuse pattern of three means that there will be a group of three cells using different frequencies. This pattern group of three repeats in the network in a way that two co-channel cells are not located adjacent to each other.

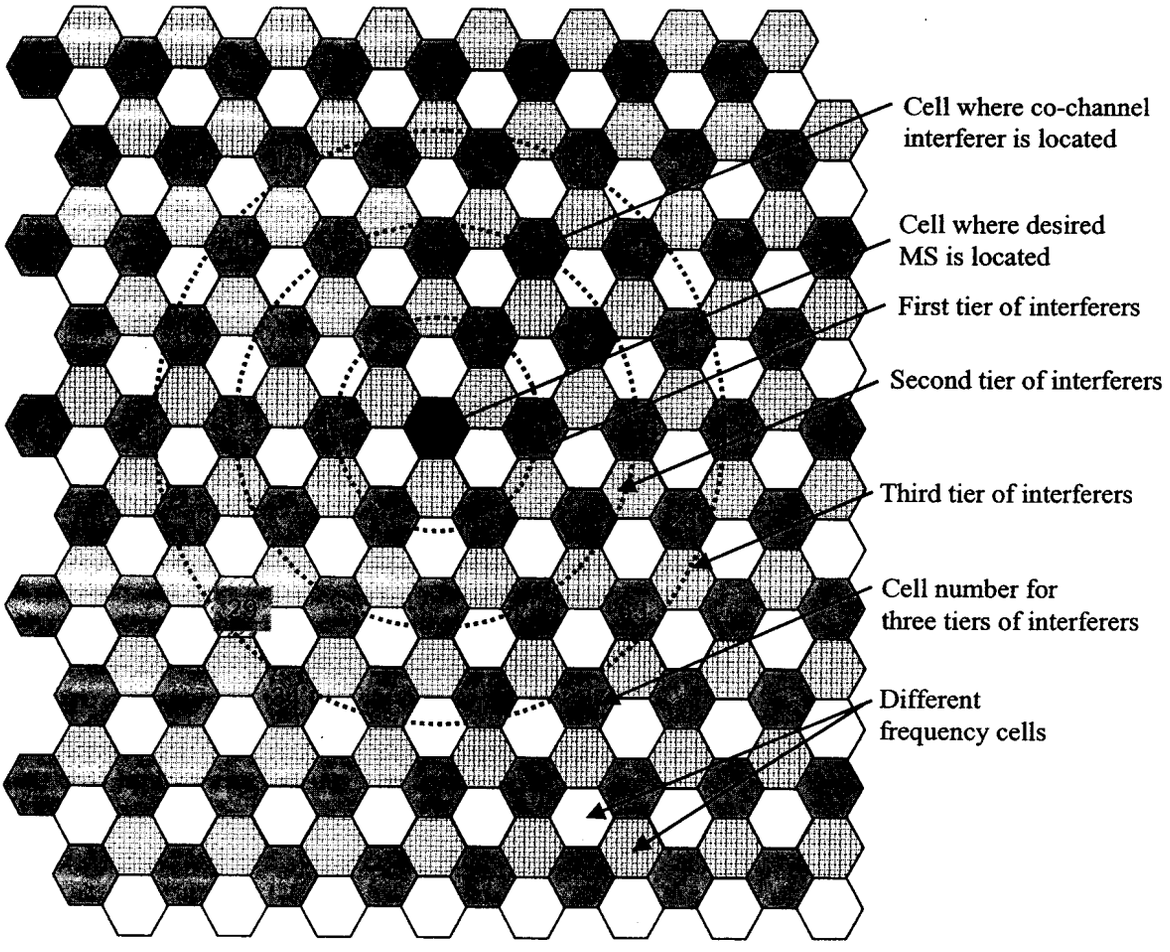

Figure 1: Network geometry with a frequency reuse factor of three.

A network with a frequency reuse pattern of one is shown in Figure 2. The desired user cell is shown in the middle, and the cell numbers are also indicated in the figure. The same frequency is reused in all the cells. This is the tightest reuse pattern with the highest interference and requires sectorization and/or adaptive arrays [50].

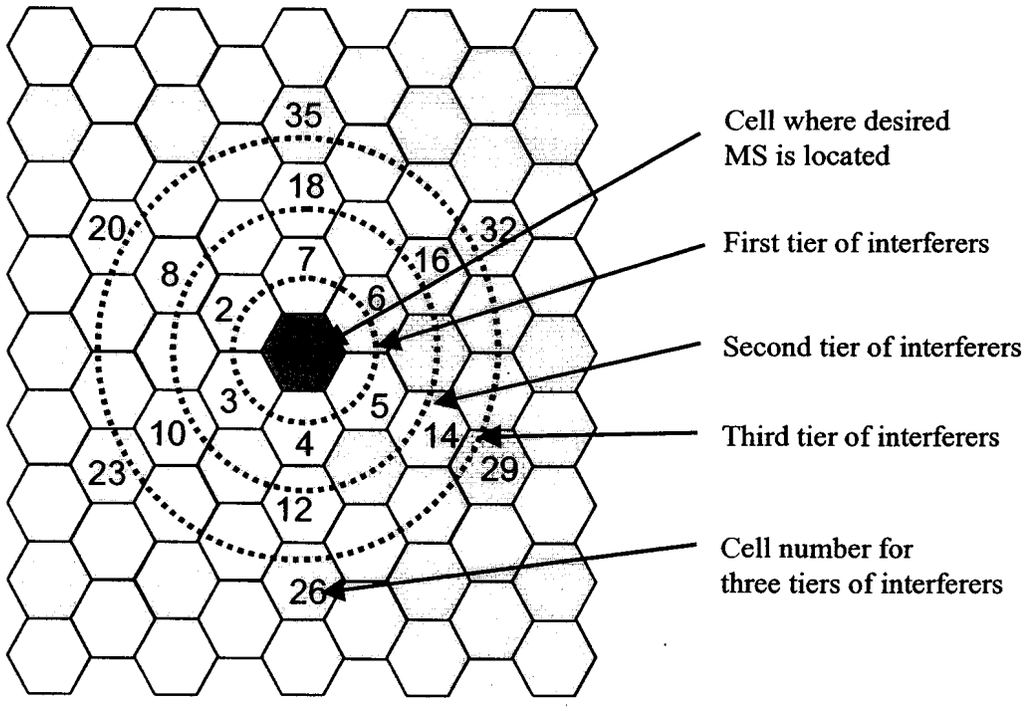

Figure 2: Network geometry with a frequency reuse of one.

One method to further increase the capacity is to have multiple users operating on the same frequency in the same cell [5]. The same cell users are separated from each other by reducing the unwanted interference by means of adaptive pattern shaping. This is called space division multiple access, where user spatial channels are created. This can be in addition to frequency and time channels.

2.3 Array Beamforming Techniques and Configurations

This section discusses different array beamforming techniques as well as array spatial configurations used with the beamforming techniques.

2.3.1 Beamforming Techniques

In this section different array beamforming techniques will be discussed. The beamforming techniques are switched multibeam, phased array beamforming and adaptive array beamforming.

2.3.1.1 Switched Multibeam

A number of fixed beams can be formed by adding a Butler matrix to the output ports of an antenna array [51]. An NxN Butler matrix will form N beams. For example, a 4x4 Butler matrix will form four beams in directions -45°, -15°, 15° and 45°. A four element

beamforming system is shown in Figure 3. In the multibeam system, the beam giving the best signal at the mobile on the downlink and best signal from the mobile on the uplink is selected. The higher directivity of a multibeam antenna compared to a sectorized antenna results in a lower level of interference received at the base station from undesired mobiles. The interference to mobiles on the downlink is also reduced. This allows for an increase in the number of mobiles that can be supported with a certain signal to interference level compared to a sectorized system [52,53].

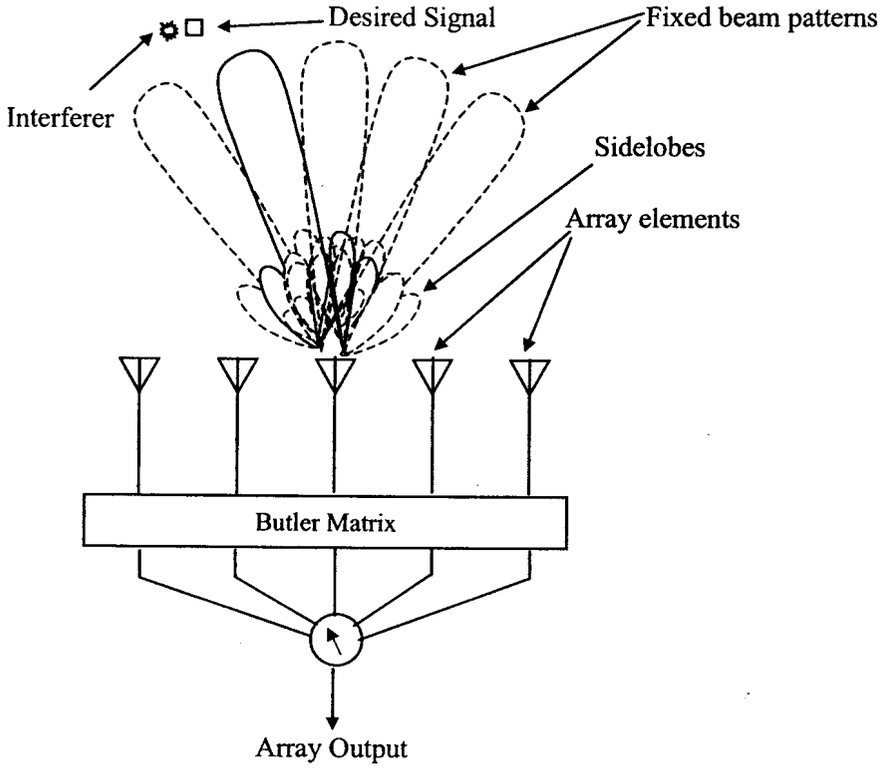

Figure 3: Array forming a number of fixed beams using a Butler matrix beamformer.

2.3.1.2 Phased Array Beamforming

A phased array has more flexibility in beamsteering direction than the multibeam system. The beam is formed by multiplying the signals from each element by a linear phase taper to steer the beam in the direction of the desired signal [51], as shown in Figure 4. An amplitude taper can also be applied to the array elements in order to reduce the sidelobe levels. This will increase the array beamwidth, determined mainly by the number of elements and the spacing between elements. The elements must be spaced close enough to

prevent grating lobes[21], which is a function of the scanning angle. Thus the more the beam is scanned away from boresight, the closer the elements need to be to prevent grating lobes. An element spacing of half a wavelength at the highest frequency is typically used [16].

The ability to separate an interferer from the desired signal depends on the beamwidth of the array. Reduction of the signal of an interferer at an incidence angle less than half a beamwidth away from the desired signal is difficult with a phased array. This is aggravated by the presence of multipath. In addition, if the desired signal multipath angular spread is wider than the array beamwidth, the total received desired signal will be reduced [16]. This will be described in detail in sections to follow.

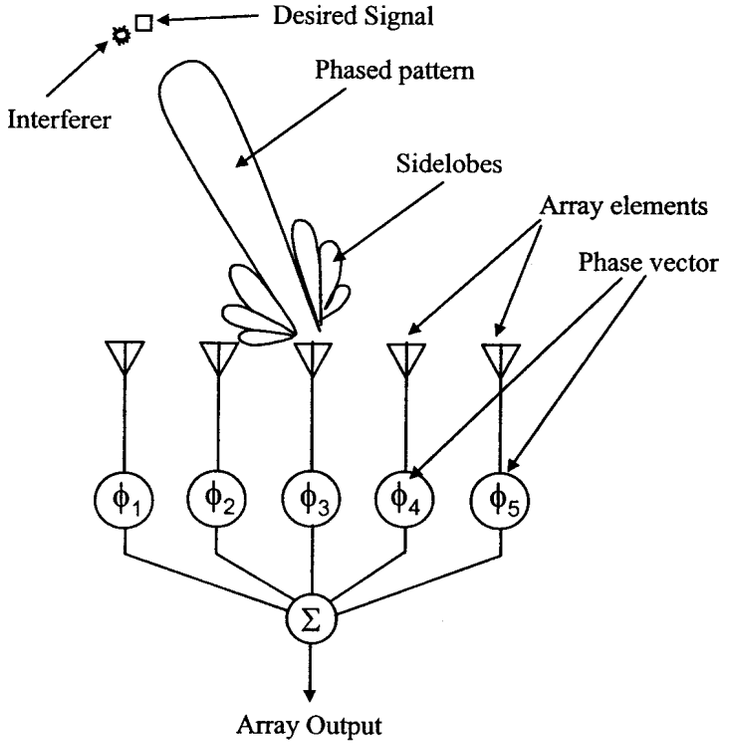

Figure 4: Phased array beam formed in the direction of the desired signal.

[21] Large antenna element spacing can result in multiple main antenna beams (grating lobes) in undesired directions due to phase ambiguities between elements.

2.3.1.3 Adaptive Array Beamforming

Given certain optimization criteria, the adaptive array matches its beamshape to the incoming signal multipath wavefront by multiplying the element signals with a complex weight vector, as shown in Figure 5. The beam is usually formed such that the desired signal to interference plus noise is maximized. The array aims to include all the multipath components of the desired signal, while minimizing all the multipath components from the interferers. The array must track the rapidly fading multipath signal by changing the complex weight vector accordingly with techniques such as least mean squares (LMS) and recursive least squares (RLS) [54].

Since the array adapts the beam to the multipath environment, the elements can be spaced far apart. This will reduce the correlation of signals received at the elements and increase the ability of the array to discriminate between the desired and interfering signals, even if they are in the same direction [2]. The smaller the angular spread, the wider the inter-element spacing needs to be in order to separate the signals. The inclusion of all the multipath signals leads to an M-fold diversity gain, where M is the number of array elements [16].

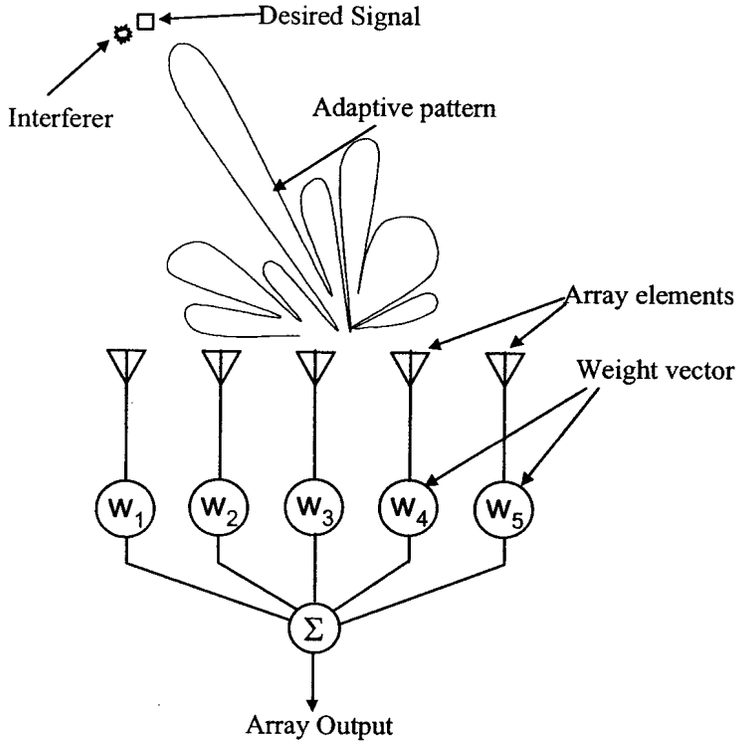

Figure 5: Adaptive array adapting its beam pattern to maximize the signal in the direction of the desired signal, while minimizing it in the direction of the interferer.

2.3.2 Array Geometry and Array Vector

The previous section discussed different beamforming techniques. Each of the beamformers requires an antenna array system. The uniform linear array (ULA) and circular array configurations are used in this thesis and will be discussed next.

The geometry of a uniform linear array is shown in Figure 6. The array consists of M elements orientated in a straight line and spaced a distance Δ apart.

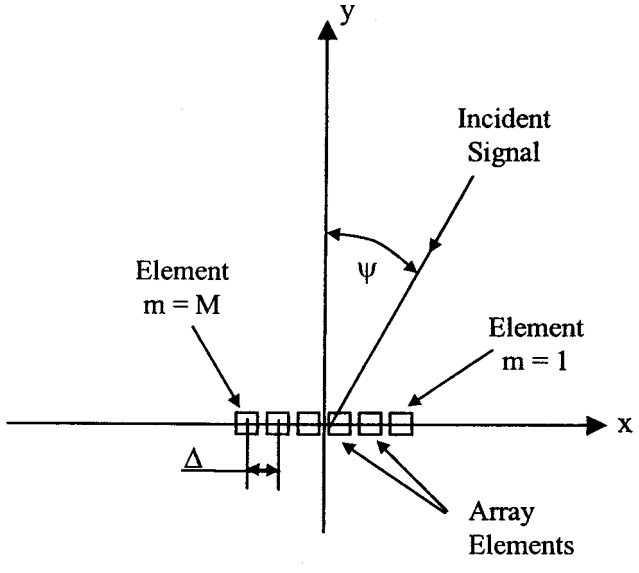

Figure 6: Uniform linear array geometry.

The array vector is [51]:

$$\mathbf{A} = F(\psi)\left\{1, e^{j\frac{2\pi}{\lambda}\Delta\sin\psi}, \ldots, e^{j\frac{2\pi}{\lambda}(M-1)\Delta\sin\psi}\right\}^T \quad (1)$$

where $F(\psi)$ is the element pattern, λ is the carrier wavelength, Δ is the element spacing and T is the transpose. A circular array[22] is shown in Figure 7, with $m \in \{1,\ldots,M\}$ the element number and M the total number of elements.

[22] Also referred to as a cylindrical array.

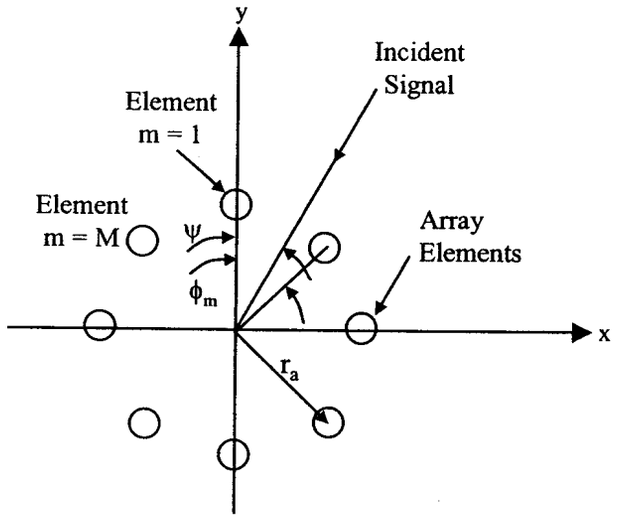

Figure 7: Circular array geometry.

The radius of the array is r_a, given by:

$$r_a = \frac{\Delta}{2\sin\left(\frac{\pi}{M}\right)} \tag{2}$$

where Δ is the spacing between the elements and M is the number of array elements. The angle ϕ_m between the x- axis and each element is given by:

$$\phi_m = \frac{2\pi(m-1)}{M} \tag{3}$$

The array vector for a signal arriving from angle Ψ is given by [16]:

$$\mathbf{A} = \left\{ F(1,\psi)\, e^{-j\frac{2\pi}{\lambda}(r_a \cos[\psi])}, \ldots, F(M,\psi)\, e^{-j\frac{2\pi}{\lambda}\left(r_a \cos\left[\psi - \frac{2\pi(M-1)}{M}\right]\right)} \right\}^T \tag{4}$$

where $F(m,\psi)$ is the element pattern.

2.3.3 Array Element Patterns

The network simulations in later chapters assume a tri-sectored network. The element pattern $F(\psi)$ that will be used in the TDMA reverse link network simulations of chapter 1 is shown in Figure 8.

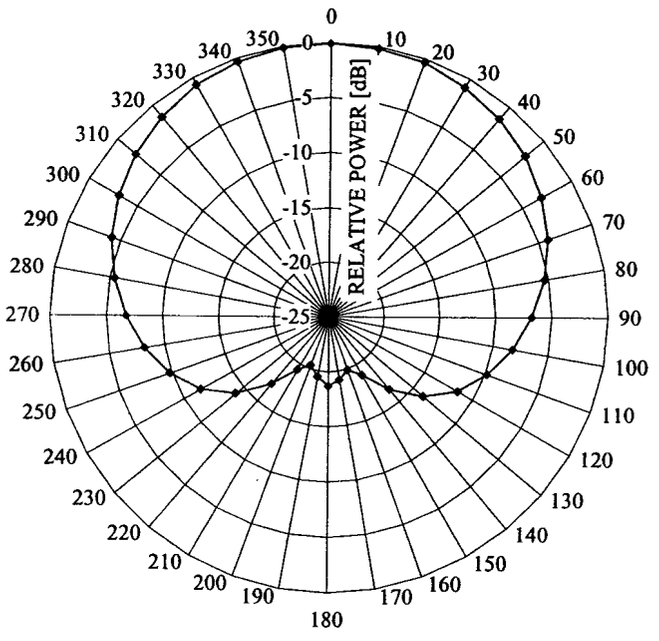

Figure 8: 120 degree element pattern.

In the range increase investigation of adaptive and phased arrays in chapter 1, a cardoid element pattern was used for the circular array elements. The cardoid pattern for the m-th element in the circular array is [16]:

$$F(m,\psi)=\sqrt{2}\cos\left[\frac{\pi}{4}\left(\cos\left\{\psi-\frac{2\pi(m-1)}{M}\right\}-1\right)\right] \qquad (5)$$

The cardoid element pattern is shown in Figure 9. The pattern has a maximum at boresight with no backlobe.

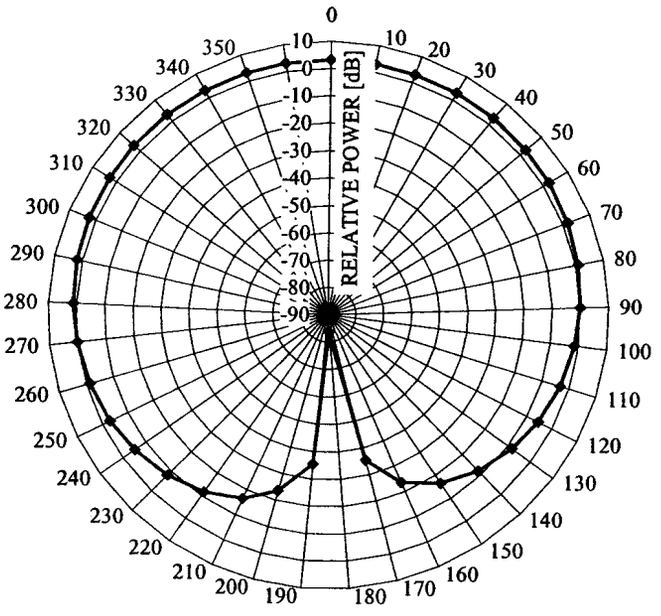

Figure 9: Cardoid element pattern.

2.4 Propagation Channel Models

In this section the propagation channel models that will be used to simulate the fading conditions between the base station and the mobile are discussed. A signal may experience two types of fading, fast and slow fading. Fast fading is due to scattering by a number of objects surrounding the mobile. The signal will add constructively or destructively at the mobile and base station due to the specific phase and amplitude relationship between all these scattered signals. The signal changes rapidly (in and out of fades) as the mobile moves around.

The second type of fading is called slow fading. Slow fading is the long-term variation of the signal due to attenuation by large objects, such as buildings or houses.

2.4.1 Fast Fading

Fast fading will be discussed in this section. Fast fading is the short-term variation of the signal at the mobile or base station due to scattering by objects surrounding the mobile or the base station.

2.4.1.1 Multipath Model

In a typical multipath environment, the mobile is surrounded by a number of scatterers. The signal is reflected, rotated in polarization, scattered and attenuated by these scatterers. The scattered signals will reach the base station with different amplitudes, incidence angles and polarizations[23]. In the case where the base station is taller than the buildings, the incidence angles will fall inside a certain angle sector, called the angular spread, as depicted in Figure 10

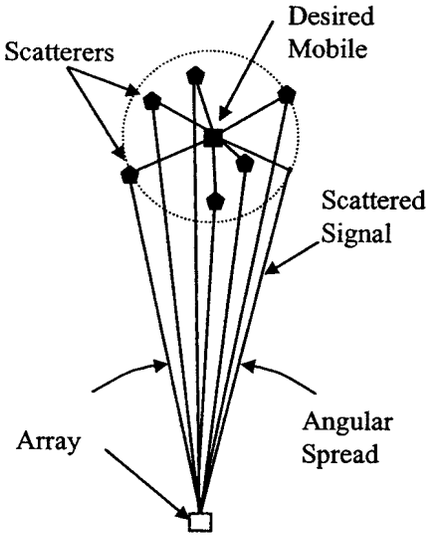

Figure 10: Multipath signals impinging on base station array.

Consider the single scattering multipath geometry[24] as shown in Figure 11. The distance between the mobile and each scatterer is $r^{s}_{d,z,k}$, where d is the mobile number, z is the cell number and k is the scatterer number. The angle between the y-axis and each scatterer is $\phi^{s}_{d,z,k}$ and the range between each scatterer and the center of the array is $r^{e}_{d,z,k}$. The distance between the mobile and the boresight of the array is $r^{c}_{d,z}$. The incidence angle relative to the array boresight of the k^{th} scatterer is $\psi_{d,z,k}$. The total distance $r^{t}_{z,za,d,k}$ between mobile, scatterer and array is a combination of the two distances:

[23] Similar to [4],[24],[32],[46],[56] the effect of polarization was not considered in this thesis.
[24] The single scattering model is not valid for all environments and base station/mobile configurations. It is stated in [22] that it is reasonable to believe that a single scattering model can be used in environments where the base antenna is high in comparison with the surrounding buildings and hills, and where there are relatively few distinct high buildings and hills at longer distances from the base station.

$$r^{t}_{z,za,d,k} = r^{e}_{z,d,k} + r^{s}_{z,za,d,k} \quad (6)$$

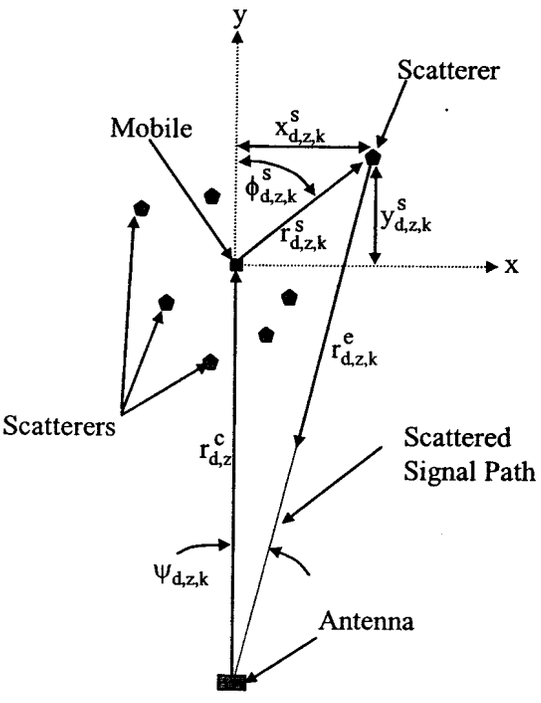

Figure 11: Geometry of multipath environment.

The multipath geometry of the desired signal and an interferer is shown in Figure 12, where the incidence angle between the array boresight and the interferer is $\psi^{c}_{d=2,z}$.

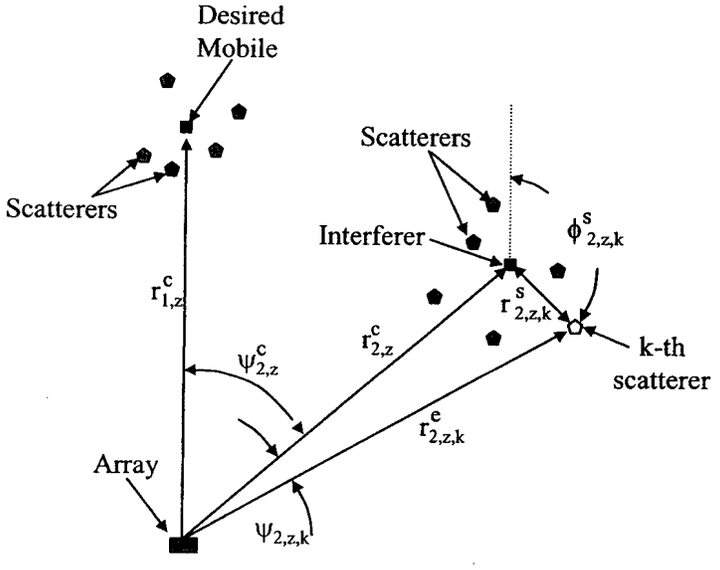

Figure 12: Geometry of desired signal and interferer multipath signals.

The multipath geometry for an interferer in an adjacent cell is shown in Figure 13, with the angle between the array boresight and the interferer in cell z = 2 is $\psi^{c}_{d=2,z=2}$.

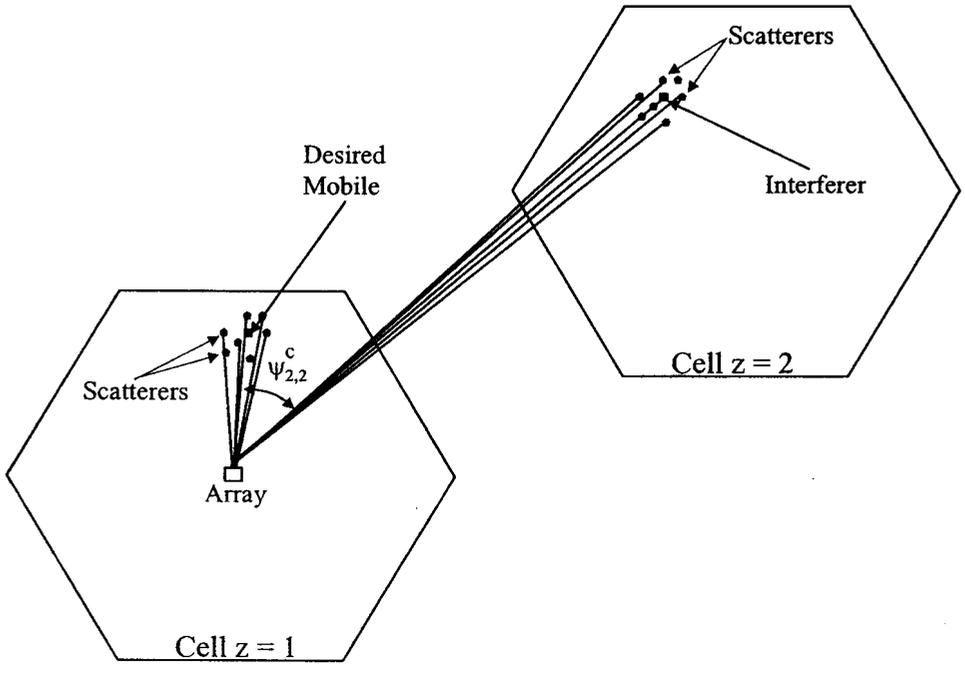

Figure 13: Multipath geometry for an interferer in an adjacent cell.

Each multipath component is considered to be a plane wave, arriving from a discrete direction and with a discrete time delay. The time-variant propagation vector[25] channel impulse response between the d^{th} mobile in cell z and antenna array in cell za [46,55,56], is:

$$\mathbf{h}_{z,za,d}(t) = \sqrt{\frac{1}{\rho_{z,za,d}(t)(4\pi r_0)^2}} \sum_{k=1}^{K} \frac{\xi_{z,za,d,k}(t)\sqrt{F(\psi_{z,za,d,k}(t))}\,\delta(t-\tau_{z,za,d,k}(t))}{\sqrt{\left(\frac{r^{t}_{z,za,d,k}(t)}{r_0}\right)^{\gamma}}} \quad (7)$$

$$e^{j\varphi_{z,za,k,d}(t)}\mathbf{A}(\psi_{z,za,d,k}(t))$$

where, $\rho_{z,za,d}$ is the log-normal[26] shadowing loss, $F(\psi_{z,za,d,k})$ is the array element pattern, $\xi_{z,za,d,k}$ is the amplitude of the signal scattered from the k^{th}-object (or closely located group of objects), $\mathbf{A}(\psi_{z,d,k})$ is the array response vector in the direction of arrival $\psi_{z,za,d,k}$

[25] A vector channel model as defined in [46] includes the angle of arrival. The vector here refers to the array response vector.
[26] Random variable in dB with a zero mean normal distribution.

of the k^{th} -scattered signal , δ is the Dirac-delta function and $r^{t}_{z,za,d,k}$ is the total distance between the mobile, scatterer and array. The delay and phase between the mobile and the k^{th}-scatterer plus between the k^{th}-scatterer and the center of the array is $\tau_{z,za,d,k}$ and $\varphi_{z,za,d,k}(t)$ respectively. Equation (7) can be written in a simplified form as:

$$\mathbf{h}_{z,za,d}(t) = \sum_{k=1}^{K} \sqrt{G_{z,za,d,k}(t)}\, \delta(t-\tau_{z,za,d,k}(t))\, e^{j\varphi_{z,za,k,d}(t)}\, \mathbf{A}(\psi_{z,za,d,k}(t)) \qquad (8)$$

where $G_{z,za,d,k}(t)$ is the path gain[27] given by:

$$G_{z,za,d,k}(t) = \frac{F(\psi_{z,za,d,k}(t))\ \xi^{2}_{z,za,d,k}(t)}{\rho_{z,za,d}(t)\ (4\pi r_0)^2 \left(\dfrac{r^{t}_{z,za,d,k}(t)}{r_0}\right)^{\gamma}} \qquad (9)$$

The amplitude $\xi_{z,za,d,k}$ can be modeled as a fixed or Rayleigh distributed random variable [56]. In the case where it is modeled as a Rayleigh distributed random variable, each scatterer actually consists of a group of scatterers located close (relative to the signal bandwidth) to each other. The case of flat Rayleigh fading is obtained when there is only a single scatterer group (K=1) [50].

2.4.1.1.1 Circular Vector Channel Model

The circular vector channel model is described in this section [25,46]. The geometry of this model for a single mobile is shown in Figure 14. It consists of K scatterers uniformly (with respect to area) distributed in a circular area with radius r^{s}_{max}.

[27] The same terminology as in [22] is used for this term, i.e. path gain.

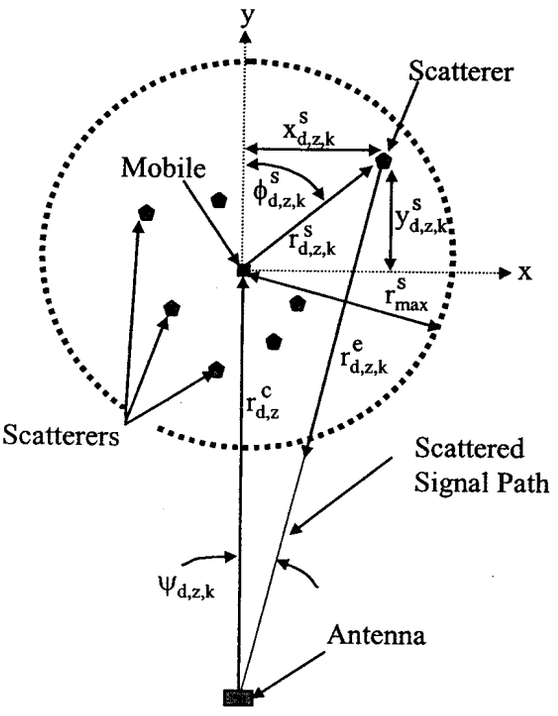

Figure 14: Geometry of the circular vector channel model.

Once the scatter locations have been determined, the propagation channel transfer function given in section 2.4.1.1 can be calculated. In [16] it was assumed that the signal is scattered equally in power by all the scatterers. This amplitude $\xi_{z,za,d,k}$ is then given by:

$$\xi_{z,za,d,k} = \frac{1}{\sqrt{K}} \tag{10}$$

where r_0 is a reference distance [56]. This model was used in the simulations of Chapter 3. The phase shift $\varphi_{z,d,k}$ is uniformly distributed between 0 and 2π [16]. Using the above assumptions, the path gain becomes:

$$G_{z,za,d,k}(t) = \frac{F(\psi_{z,za,d,k}(t))}{K\,\rho_{z,za,d}(t)\,(4\pi r_0)^2 \left(\frac{r^t_{z,za,d,k}(t)}{r_0}\right)^{\gamma}} \tag{11}$$

2.4.1.1.2 Angular Incident Power Distribution

The scattered signal from each of the K objects can either have a constant amplitude or a Gaussian amplitude distribution given by:

$$p(\xi) = \frac{1}{\sqrt{2\pi}\sigma} e^{\left(\frac{-\xi^2}{2\sigma^2}\right)} \tag{12}$$

with a standard deviation of:

$$\sigma = \sqrt{\frac{1}{K}} \tag{13}$$

and with a transmit signal power of 1. This Gaussian amplitude distribution was used in the simulations of section 5.1.2. The phase from each scatterer is $e^{j2\pi\varphi}$, with φ a uniform random variable between 0 and 1. The total signal received at the base station is the sum of all the complex signals from the scatterers and has real and imaginary components that are Gaussian distributed with an envelope that is Rayleigh distributed [11]. The incidence angle ψ is Gaussian distributed with zero mean and with a PDF given by [50]:

$$p(\psi) = \frac{1}{\sqrt{2\pi}\sigma_{as}} e^{\left(\frac{-\psi^2}{2\sigma_{as}^2}\right)} \tag{14}$$

where σ_{as} is the standard deviation of the angular spread or half of the angular spread.

2.4.2 Slow Fading

A mobile signal shadowed from the BTS by a large object, such as a building or bridge, will experience a significant attenuation. This attenuation is typically referred to as slow fading, which is a large scale variation superimposed on the small scale fading or fast fading. The duration of a slow fade is typically the time the mobile moves 10 to 30 m, which corresponds to the typical length of small to medium sized buildings. A typical slow fading variation superimposed on a fast fading pattern is shown in [50].

Slow fading is generally modeled as a log-normal distribution [12]. This means that the slow fading in decibels has a Normal or Gaussian distribution, with probability density function given as [37]:

$$p(\rho_{z,za,d}^{dB}) = \frac{1}{\sqrt{2\pi}\,\sigma_{sf}} e^{\left(-\frac{\left\{\rho_{z,za,d}^{dB}\right\}^2}{2(\sigma_{sf})^2}\right)} \tag{15}$$

where $\rho_{z,za,d}^{dB}$ is the slow fading random variable in dB. The PDF has a zero mean and standard deviation σ_{sf}. A typical slow fading histogram with a standard deviation of 8dB is shown in Figure 15.

Power control normally compensates for slow fading. If the received signal at the mobile is weak due to slow fading, the base station will transmit more power to the specific mobile. In a TDMA system, each user has a particular timeslot. The power for the specific timeslot is increased or decreased depending on the fading attenuation. In CDMA, the power (or forward gain) of a specific traffic channel (Walsh spreading code) is increased or decreased according to the slow fade before all the spreading codes are summed together.

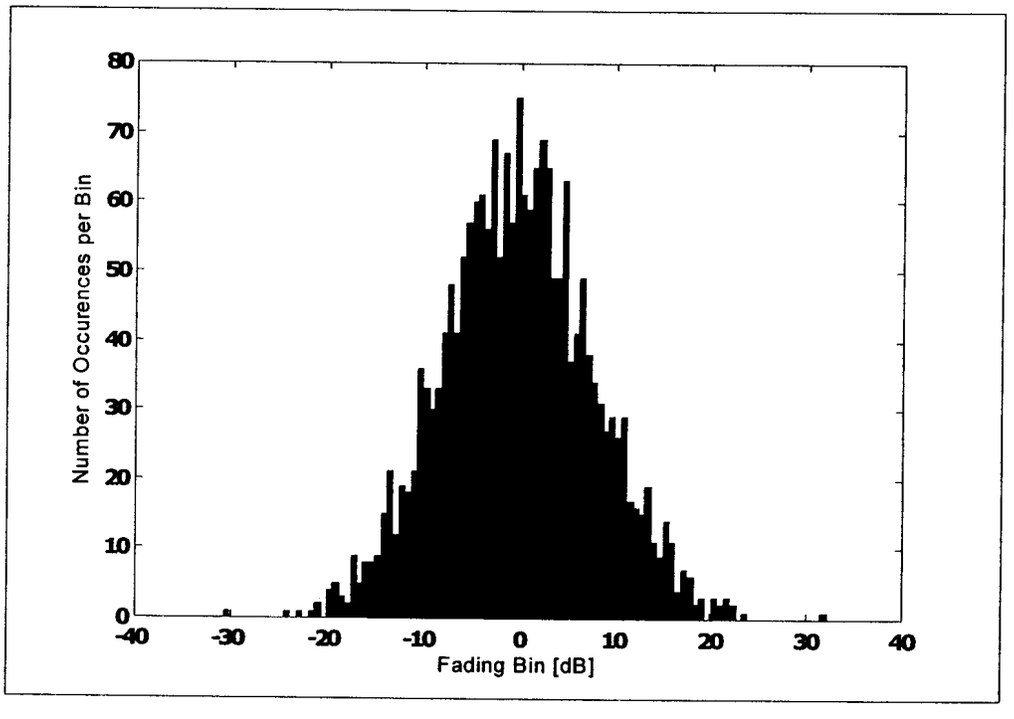

Figure 15: Histogram (PDF) of slow fading loss with a standard deviation of 8dB.

2.5 Spatially Distributed Array Definition

The concept of the spatially distributed array is presented in this section, as well as the practical implementation considerations for this configuration

2.5.1 Distributed Array Concept

A conventional tri-sectored network consists of three 120° sector antennas, with 120° between the boresights of the antennas. In order to reduce (beyond that of sectorization)

the out of cell co-channel interference signals on the uplink (operating on the same frequency and timeslot as the desired mobile in TDMA and GSM systems) and towards mobiles on the downlink, adaptive arrays can be used [1,2,3]. The adaptive arrays are placed at the same locations as the sectorized antennas in the cell (see Figure 16), with element patterns similar to the sectorized antenna pattern.

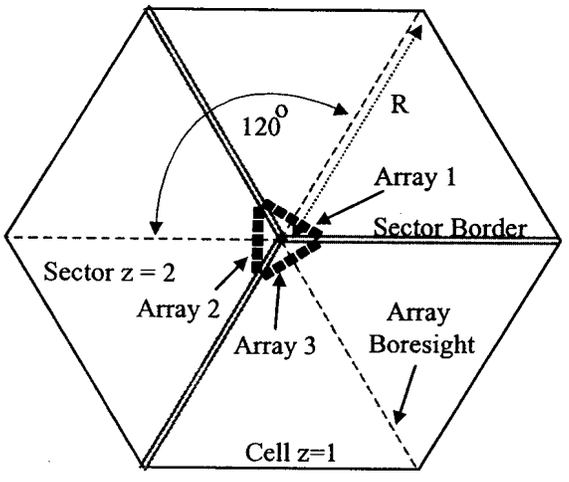

Figure 16: Three arrays at the center of the cell.

With this adaptive array configuration, the capacity can be increased further by allowing multiple co-channel users in the same sector as the desired mobile [4,5,6]. Similar to a tri-sectored configuration, each sector has different frequencies. The users in each sector are isolated from each other in angle with the adaptive array by reducing the received energy from the co-channel interferers, while maximizing the signal of the desired co-channel users. This creates spatial channels for the users, called space division multiple access (SDMA). However two users that have nearly the same incidence angle in an environment with a small angular spread are difficult to be spatially isolated from each other and have to be assigned to different channels (frequency or time) [5].

The spatial resolution required to discriminate between users with a small difference in incidence angle in a narrow angular spread environment can be improved by employing an adaptive array at every other corner of a hexagonal cell. The concept of placing base stations at the edge of a hexagonal cell was first proposed in [7,8,9]. However, the technique presented in this thesis differs from [7] in that adaptive arrays are used on the base stations instead of 120° overlapping sectorized antennas. It differs from [8,9] in that

combined beamforming of the arrays is considered instead of selection diversity. The three arrays on every other edge of a hexagonal cell form sub-arrays of one large array system, where the steering vector of the array system is optimized to yield the best signal to interference ratio for all co-channel users in the same-cell.

The array system is able to spatially discriminate between co-channel users in a two-dimensional plane, as each array has a different viewing angle towards the users. A desired user may be closely located in angle to an interferer as seen from one array, while from a different viewing angle, another array might be able to spatially separate the user from the interferer. The result is that even more co-channel users can operate in the same cell compared to conventional methods in a narrow angular spread environment with closely spaced antenna elements.

2.5.2 Conventional Array Geometry

The performance of the distributed array will be compared to the conventional array, and therefore the conventional array geometry must be defined. The geometry of the conventional arrays at the center of the cell is shown in Figure 17. There are three antenna arrays, each with M antenna elements and with an element pattern covering a nominal angle of ± 60°. The angle between the boresight of each array $\kappa \in \{1,2,3\}$ and scatterer $k \in \{1,2,...,K\}$ is $\psi_{z,za,\kappa,d,k}$, where z is the cell number in which mobile d is located and za is the cell number where the array is located.

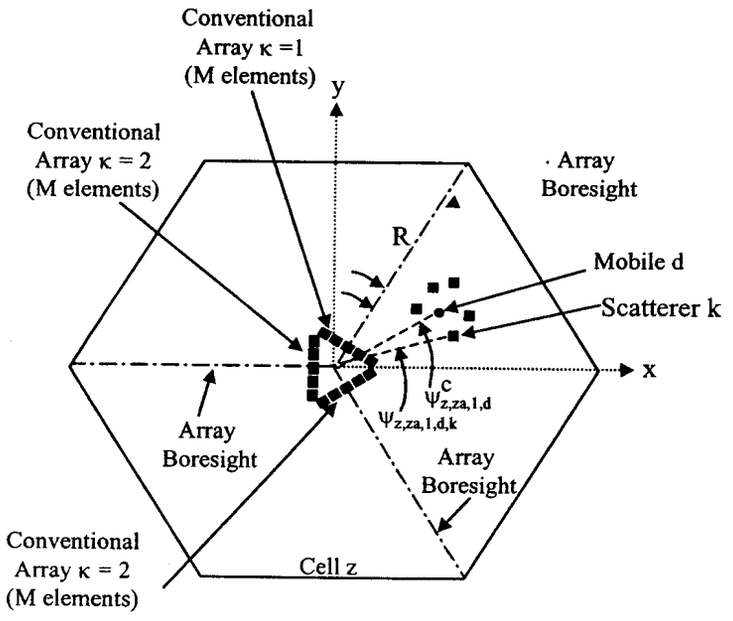

Figure 17: Geometry of the conventional antenna arrays at the center of a hexagonal cell.

R is the cell radius, which is the distance between the center of the cell and the furthest point of the hexagonal cell.

2.5.3 Distributed Array Geometry

The geometry of three sub-arrays at alternate corners of a hexagonal cell is shown in Figure 18. Each of these antenna sub-arrays has M antenna elements. Each antenna sub-array pattern covers a nominal angle of $\pm 60°$. The angle between the boresight of each sub-array $\kappa \in \{1,2,3\}$ and scatterer $k \in \{1,2,...,K\}$ is $\psi_{z,za,\kappa,d,k}$, where z is the cell number in which the mobile d is located and za is the cell number where the distributed array is located.

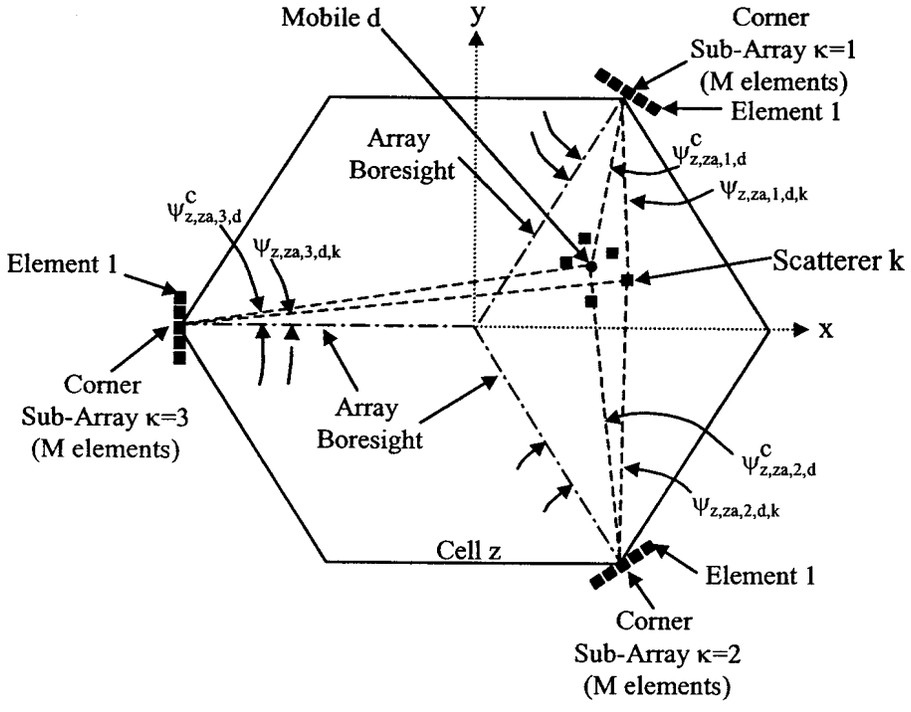

Figure 18: Distributed array geometry.

2.5.4 Practical Implementation Considerations

The fact that the sub-arrays are located at the edges of the cell and thus separated far apart, as well as the fact that they have to function as part of a larger array, results in practical limitations and implementation factors which must be taken into consideration. The following factors: 1) cell size limitation, 2) effective processing of the signals arriving at all the antenna elements, and 3) power control are discussed in sections 2.5.4.1 to 2.5.4.3.

2.5.4.1 Cell Radius of Distributed Array versus Array at the Cell Center

The distributed sub-arrays are located at the edges of the cell. A mobile at the edge of the cell will have a mobile to sub-array separation distance that can be up to twice the separation distance for a standard sectorized cellsite configuration. With a propagation path-loss coefficient of 3.5 (typical for an urban environment [5]) and twice the distance, an additional pathloss of 10.5dB can be encountered between the mobiles and the sub-arrays .

On the other hand, the directivity of the sub-arrays is higher than the directivity of a standard tri-sector antenna. The directivity of distributed sub-arrays varies as a function of the distribution of the mobiles. The mean and standard deviation of the difference in azimuth directivity between each of the sub-arrays and a sector antenna with a 105° half-power beamwidth, were calculated as 5.04dB and 1.26dB for sub-array 1, 4.75dB and 1.22dB for sub-array 2 and 4.77dB and 1.13dB for sub-array 3, respectively. This was calculated with a total of 500 iterations using different mobile positions for each iteration, nine element arrays and seven mobiles uniformly distributed over the whole cell area. The minimum (mean minus standard deviation) difference in azimuth directivity between the adaptive sub-arrays and the sector antenna is approximately 3.5 dB. This gain difference allows the adaptive sub-array range to be 1.26 times the range of the sectorized antenna, with a pathloss exponent of 3.5. Now, without increasing the mobile maximum transmit power or base station sensitivity on the uplink (or mobile sensitivity and base station power on the downlink), the maximum noise limited cell radius of the distributed array can only be 0.63 times (1.26 divided by 2) the maximum noise limited radius of the centrally located sectorized cellsite.

Therefore, due to the fact that the distributed sub-arrays are located at the edges of the cell, the cell radius of the adaptive distributed array will be less than the cell radius of a traditional tri-sector cellsite. This radius difference is a function of the pathloss exponent.

2.5.4.2 Joint Adaptive Beamforming with Spatially Removed Arrays

The optimum steering vector is determined from signals present at all the sub-array elements. In order to determine the steering vector, the baseband signals of all the antenna elements (all the sub-arrays) are added together after being weighted. Using the least mean squares method, this output signal is then compared to a known signal and a cost function is determined as described in section 2.7.1.1.1. The baseband signals can be transmitted to a central processing unit where the optimum weight vector can be determined. However, this will result in a huge amount of data that has to be transmitted to the processing unit.

This can be overcome by first multiplying the baseband signals of each sub-array with an optimum weight vector for each desired user (determined in the previous iteration), adding the result together for each desired user and thus forming the vector at each sub-array:

$$Y_{\kappa}(nT_s) = \mathbf{W}_{\kappa}^{H}\,\mathbf{X}_{\kappa}(nT_s) \qquad (16)$$

where $\kappa \in [1,2,3]$ is the sub-array number, **W** is the weight vector and **X** is the array signals downconverted to baseband at each array. The resultant output for each desired user must then be transmitted to a central processing unit, where the output signal from each base station for each desired user is coherently summed. The total resultant output for each user is compared to the known sequence of each desired user and a complex cost function (complex value) is determined for each desired user. The cost functions are then transmitted to all three base stations. At each base station, the updated steering vector for each user is determined. The resultant steering vector is identical to the steering vector that can be obtained when all the antenna element data is transmitted to and processed in one central location.

The three array output signals must be coherently combined in time and phase, otherwise the desired SINR will decrease. The delay between the three signals must be accurately aligned using for example delay lines at the central receiver. The phase can be aligned by using for example a pilot signal transmitted (via a cable or oprical fibre) from each sub-array (together with the traffic signal) and then changing the phase of the three signals (from the three sub-arrays) with complex digital multipliers until a maximum signal is observed from the combined signals

2.5.4.3 Power Control Implementation

In this section a practical method implementing power control for the distributed array system is presented. Three timeslots are required for power control. During timeslot 1 only sub-array 1 is receiving. The power of all mobiles are adjusted for sub-array 1, based on the received up-link signal, which is a function of distance and fading between the mobiles and sub-array 1. Power control in timeslots 2 and 3 is done for sub-arrays 2 and 3 respectively. The same information is transmitted by all mobiles during all three timeslots.

2.5.5 Distributed Array Power Control in Simulations

In the simulations of chapters 1 and 2, the following two power control methods are used:

1. The power is controlled by the nearest sub-array, as described in 2.5.5.1

2. The power is controlled by the sub-array receiving the strongest signal, including distance and slow fading, as described in 2.5.5.2.

2.5.5.1 Range Power Control

In the absence of slow fading, it is assumed that the power for the co-channel users is controlled by the closest sub-array [37]. If the power control distance for mobile d in cell z and array in cell za is denoted by $r^{c,pc}_{z,za,d}$, the path gain can be written as (see Figure 14):

$$G_{z,za,\kappa,d,k}(t) = \frac{\lambda^2 \xi^2_{z,za,\kappa,d,k}(t)}{(4\pi r_0)^2 \left(\frac{r_{z,za,\kappa,d,k}(t)}{r_0 r^{c,pc}_{z,za,d}(t)} \right)^{\gamma}} F(\psi_{z,za,\kappa,d,k}(t)) \qquad (17)$$

where κ is the sub-array number, $F(\psi_{z,za,\kappa,d,k})$ is the antenna element normalized power pattern (see section 2.3.3), ψ is the angle of the mobile relative to the antenna boresight, γ is the pathloss exponent and r_0 is the free space pathloss reference distance. In the presence of slow fading, power can either be controlled by the closest sub-array or by the sub-array receiving the strongest signal. In the case where the power is controlled (for mobile d in cell z) by the closest base station, the path gain is (see Figure 14):

$$G_{z,za,\kappa,d,k}(t) = \frac{\lambda^2 \xi^2_{z,za,\kappa,d,k}(t)}{(4\pi r_0)^2 \left(\frac{r_{z,za,\kappa,d,k}(t)}{r_0 r^{c,pc}_{z,za,\kappa,d,k}(t)} \right)^{\gamma} \rho_{z,za,\kappa,d}(t)} F(\psi_{z,za,\kappa,d,k}(t)) \qquad (18)$$

where k is the scatter number, $\rho_{z,za,\kappa,d}$ is slow fading path loss between mobile d in cell z and array κ in cell za, $F(\psi_{z,za,\kappa,d,k})$ is the antenna element normalized power pattern (see section 2.3.3), κ is the sub-array number and r_0 is the free space path loss reference distance.

2.5.5.2 Signal Strength Power Control

In the case of power control by the array receiving the strongest signal in the presence of slow fading, the path gain is given by:

$$G_{z,za,\kappa,d,k}(t) = \frac{\lambda^2 \ \xi^2_{z,za,\kappa,d,k}(t)}{(4\pi r_0)^2 \left(\frac{r_{z,za,\kappa,d,k}(t)}{r_0 \, r^{c,pc}_{z,za,d}(t)}\right)^{\gamma} \left(\frac{\rho_{z,za,\kappa,d}(t)}{\rho^{pc}_{z,za,d}(t)}\right)} F(\psi_{z,za,\kappa,d,k}(t)) \qquad (19)$$

where $\rho^{pc}_{z,za,d}$ is the slow fading loss between mobile d in cell z and the sub-array of the controlling base station za where the received signal is a maximum, $r^{c,pc}_{z,za,d}$ is the associated range between the mobile d in cell z and array in cell za and r_0 is the free space pathloss reference distance.

2.6 Array Output Signals and Array Combining

The signals received at the array elements are presented in this section, for both narrowband and wideband (spread spectrum) systems. The multiplication of the signals by a complex weight vector is described as well as combining of all the weight multiplied signals to form one output signal for all the array elements. The extraction of the desired signal component from the wideband array signals will be described, as well as detection and combining of the strongest multipath signals. Methods of combining of the conventional array signals and distributed sub-array signals, will then be presented.

2.6.1 Narrowband Individual Array Output Signals

Assume that the base stations and arrays are synchronized. The output of each array is obtained by multiplying each of the m antenna element signals with a complex weight, and then summing the resultant signal. The sampled output of array κ ($\kappa \in [1,2,3]$) optimized for user d (d is co-channel users with $d \in [1,2,...,D]$) is [1,51,57]:

$$Y_{\kappa,d}(nT_s) = \mathbf{W}^H_{\kappa,d} \, \mathbf{X}_{\kappa}(nT_s) \qquad (20)$$

where n is the sample number, T_s is the sampling period. $\mathbf{W}^H_{\kappa,d}$ is the complex conjugate transpose of the weight vector of array κ optimized for used d, given by:

$$\mathbf{W}_{\kappa,d} = [W_{\kappa,d,1} \ W_{\kappa,d,2} \ \ldots \ W_{\kappa,d,M}]^T \qquad (21)$$

The weight vector estimation procedure is described in section 2.7. $\mathbf{X}_{\kappa}$ are the complex baseband signals (combination of the signals of all D users) at array κ, given by:

$$\mathbf{X}_{\kappa,d} = [X_{\kappa,1}\ X_{\kappa,2} \ldots X_{\kappa,M}]^T \tag{22}$$

Using a far-field approximation, the received signal at the base station antenna is a convolution of the transmit signal and the channel impulse response function in (7). The received signal at element m of array κ (or sub array κ in the case of the distributed array) in cell za is given by [56]:

$$\mathbf{X}_{za,\kappa}(t) = \sum_{z=1}^{Z}\sum_{d=1}^{D} S_{z,d}(t) \otimes \mathbf{h}_{z,za,\kappa,d}(t) + \mathbf{n}_s(t,\kappa) \tag{23}$$

where $\kappa \in [1,2,3]$ is the array number in cell za. $S_{z,d}(t)$ is the complex signal transmitted by the d^{th} co-channel in cell z user convolved with the impulse response of the base station receive filter and $\mathbf{n}_s(t,\kappa)$ is the additive white noise at the array κ elements, which is assumed to be Gaussian distributed with zero mean and variance σ_N^2. Using the propagation channel transfer function in (7), (23) can be written as:

$$X_{za,\kappa,m}(t) = \sum_{z=1}^{Z}\sum_{d=1}^{D}\sum_{k=1}^{K} \{S_{z,d}(t-\tau_{z,za,\kappa,d,k}) \sqrt{G_{z,za,\kappa,d,k}(t)}\ e^{j\varphi_{z,za,\kappa,d,k}(t)} A(m, \psi_{z,za,\kappa,d,k}(t))\} + n_s(t,\kappa,m) \tag{24}$$

where λ is the wavelength. $G_{z,za,\kappa,d,k}$ is the path gain between mobile d in cell z, base station array κ in cell za and multipath component k, given in (17),(18) and (19). Assuming an ideal receive filter and down converting the signal to baseband, the signal amplitude $S_{z,d}(t)$ in equation 24 is:

$$S_{z,d}(t) = \sum_{n=1}^{\infty} b_{z,d}(nT_b)\ p(t-nT_b) \tag{25}$$

where n is the symbol number, $b_{z,d}$ is the d^{th} user complex sequence of transmitted data symbols with period T_b and p(t) is the transmitted pulse shape.

2.6.2 Wideband (Spread Spectrum) Individual Array Output Signals

Spread spectrum systems include e.g. CDMA IS-95 and IS-2000[28] configurations with a spreading bandwidth of 1.2288 MHz. The baseband signal transmitted from the d^{th} mobile in cell z can be written as [12]:

$$S^{t}_{z,d}(t) = \vartheta_{z,d}\sqrt{P_{z,d}}\, b_{z,d}(t) c_{z,d}(t) \tag{26}$$

where $\upsilon_{z,d}$ is the voice activity factor (binary random variable with success $p_{z,d}$), $P_{z,d}$ is the controlled mobile transmit power, b is the differentially encoded information data bits of duration T_b and $c_{z,d}$ is the spreading code (1.2288 MHz bandwidth in IS-95 and IS-2000). The spreading code of user d in cell z can be written as [12]:

$$c_{z,d}(t) = \sum_{n=-\infty}^{\infty} c_{z,d}(nT_c)\, p(t - nT_c) \tag{27}$$

where p(t) is the chip pulse shape (which is assumed rectangular in the simulations to follow) and $c_{z,d}(nT_c)$ are assumed to be independent random variables with values ± 1 and with equal probability. The spread spectrum adaptive array system is shown in Figure 19.

[28] Also referred to as 1xRTT.

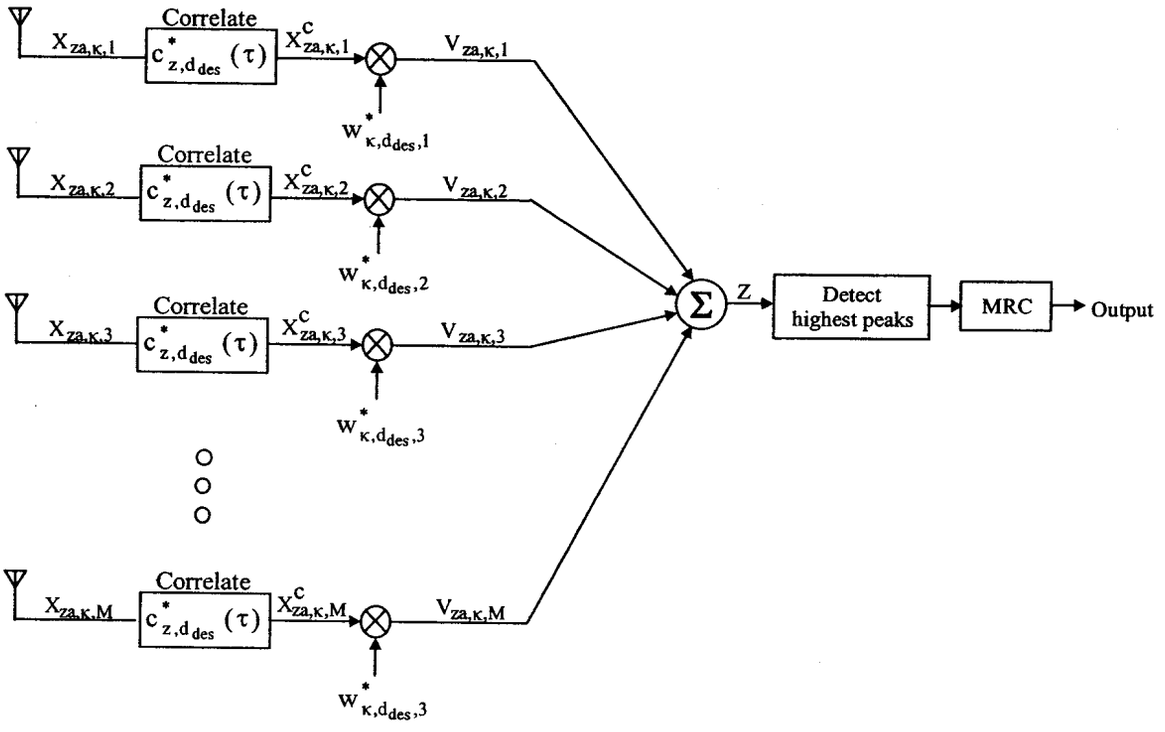

Figure 19: Spread spectrum adaptive array system.

The output of each branch m of array κ is sampled with period T_s and then downconverted to baseband to form the complex baseband signals (combination of the signals of all D users) $\mathbf{X}_\kappa$, where:

$$\mathbf{X}_\kappa(nT_s)=\left[X_{\kappa,1}(nT_s)\quad X_{\kappa,2}(nT_s)\quad \ldots\quad X_{\kappa,M}(nT_s)\right]^T \tag{28}$$

Inserting (26) in (24), the baseband received signal vector from mobile d at element m of array κ in cell za can be written as [12]:

$$X_{za,\kappa,m}(nT_s)=\sum_{z}^{Z}\sum_{d=1}^{D}\sum_{k=1}^{K}\{\vartheta_{z,d}\sqrt{P_{z,d}}\;b_{z,d}(nT_s-\tau_{z,za,\kappa,d,k})\;c_{z,d}(nT_s-\tau_{z,za,\kappa,d,k})$$

$$\sqrt{G_{z,za,\kappa,d,k}(nT_s)}\;e^{j\left\{\frac{2\pi}{\lambda}r^{t}_{z,\kappa,d,k}(nT_s)\right\}}A(m,\psi_{z,za,\kappa,d,k})\}\;+\;n_s(nT_s,\kappa,m) \tag{29}$$

Each antenna element is followed by a RAKE receiver[29], where the first processing stage is to despread the signal with the desired signal d_{des} spreading code $c_{z,d_{des}}$, i.e.

[29] Coherent combining of L multipath signals spaced integer periods apart, with n ≥ 1.

$$X^{c}_{za,\kappa,m}(nT_s, d_{des}) = \int_{-\infty}^{\infty} X_{za,\kappa,m}(nT_s - \tau)\, c^{*}_{z,d_{des}}(\tau)\, d\tau \qquad (30)$$

where X^c is the despreaded signal and z is is the cell containing the desired signal. The autocorrelation function of spreading code $c_{z,d}$ at sample time n T_s is given by (see Figure 20) [16]:

$$ACF[\tau, nT_s] = g_p\left\{1 - \frac{|\tau - nT_s|}{T_c}\right\} \qquad (31)$$

where g_p is the processing gain (ratio between the spreading code rate and the bit rate).

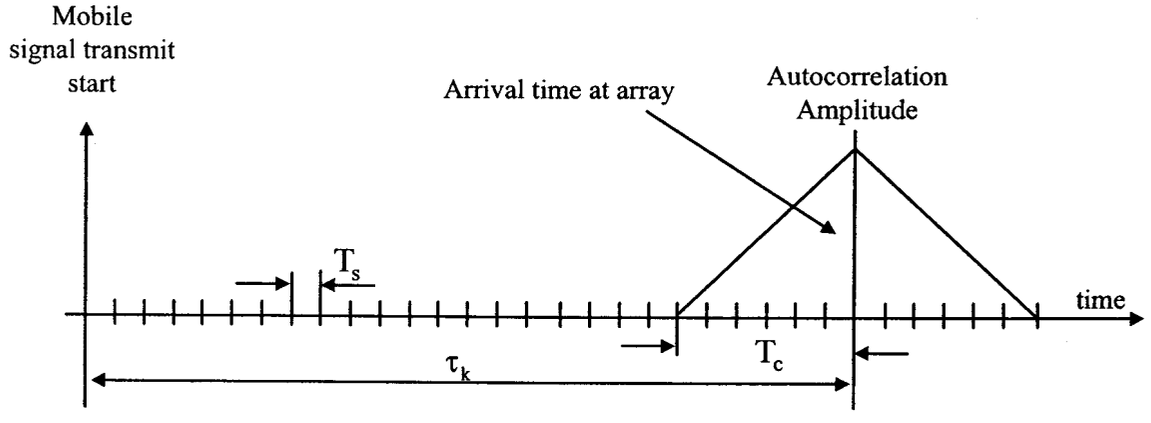

Figure 20: Autocorrelation function of k^{th} multipath component.

Using (30) and (31), the desired signal portion (portion correlating with desired signal spreading code) of (29) at time sample n T_s in cell z_{des} is:

$$X^{c,des}_{z_{des},za,\kappa,m}(n\,T_s, d_{des}) = g_p \sum_{k=1}^{K} \{\vartheta_{z_{des},d_{des}} \sqrt{P_{z_{des},d_{des}}}\; b_{z_{des},d_{des}}(n\,T_s - \tau_{z_{des},za,\kappa,d_{des},k})$$

$$\left[1 - \frac{|\tau_{z_{des},za,\kappa,d_{des},k} - n\,T_s|}{T_c}\right] \sqrt{G_{z_{des},za,\kappa,d_{des},k}(nT_s)}\; e^{j\left\{\frac{2\pi}{\lambda} r^{t}_{z_{des},\kappa,d_{des},k}(nT_s)\right\}}$$

$$A(m, \psi_{z_{des},za,\kappa,d_{des},k})\} \qquad (32)$$

The total received interference plus noise signal after despreading at time sample nT_s is:

$$X^{c,int}_{za,\kappa,m}(nT_s,d_{des}) = \sum_{\substack{d=1\\ d\neq d_{des}}}^{D}\sum_{k=1}^{K}\{\vartheta_{z,d}\sqrt{P_{z,d}}\sqrt{G_{z,za,\kappa,d,k}(nT_s)}\; e^{j\left\{\frac{2\pi}{\lambda}r^{t}_{z,\kappa,d,k}(nT_s)\right\}} A(m,\psi_{z,za,\kappa,d,k}(nT_s))\} + n_s(nT_s,\kappa,m) \quad (33)$$

The signals in (32) and (33) are then multiplied by the conjugate of a complex weight vector $\mathbf{W}_{\kappa,d_{des}}$ for optimization to the desired user d_{des}, to yield the signal vectors $\mathbf{V}^{des}_{za,\kappa,m,d_{des}}(nT_s,d_{des})$ and $\mathbf{V}^{int}_{za,\kappa,m,d_{des}}(nT_s,d_{des})$ optimized for user d_{des}. Weight estimation procedures are described in section 2.7. The components of the vectors $\mathbf{V}^{des}_{za,\kappa,m,d_{des}}(nT_s,d_{des})$ and $\mathbf{V}^{int}_{za,\kappa,m,d_{des}}(nT_s,d_{des})$ is then summed to yield the corresponding signals $Z^{des}_{za,\kappa.d_{des}}(nT_s,d_{des})$ and $Z^{int}_{za,\kappa,d_{des}}(nT_s,d_{des})$. The next step is to detect the L largest peaks (called fingers in a RAKE receiver) separated by integer multiples of the spreading code period in the desired signal $Z^{des}_{za,\kappa}(nT_s,d_{des})$. The resultant desired signal at the time of arrival of each of the fingers ($n_\ell T_s$) of the RAKE receiver is:

$$Z^{des}_{za,\kappa}(n_\ell T_s,d_{des}) = g_p\sum_{m=1}^{M}\sum_{k=1}^{K}\{\sqrt{P_{z,d_{des}}}\; b_{z,d_{des}}(n_\ell T_s-\tau_{z,za,\kappa,d_{des},k})\left[1-\frac{\left|\tau_{z,za,\kappa,d_{des},k}-n_\ell T_s\right|}{T_c}\right]\sqrt{G_{z,za,\kappa,d_{des},k}(n_\ell T_s)}\; e^{j\left\{\frac{2\pi}{\lambda}r^{t}_{z,\kappa,d_{des},k}(n_\ell T_s)\right\}} A(m,\psi_{z,za,\kappa,d_{des},k}(n_\ell T_s))\}\, W^{*}_{\kappa,d_{des}}(\ell,m) \quad (34)$$

where $W_{\kappa,d_{des}}(\ell,m)$ is the ℓ^{th} component of the weight vector and n_ℓ is the time sample number of the ℓ^{th} finger. The interference plus noise signal after weight multiplication is:

$$Z_{za,\kappa}^{int}(n_\ell T_s, d_{des}) = \sum_{m=1}^{M} \sum_{\substack{d=1 \\ d \neq d_{des}}}^{D} \sum_{k=1}^{K} \{\vartheta_{z,d} \sqrt{P_{z,d}} \sqrt{G_{z,za,\kappa,d,k}(n_\ell T_s)}\, e^{j\left\{\frac{2\pi}{\lambda} r^t_{z,\kappa,d,k}(n_\ell T_s)\right\}}$$

$$A(m, \psi_{z,za,\kappa,d,k}(n_\ell T_s))\} + n_s(n_\ell T_s, \kappa, m)] W^*_{\kappa,d_{des}}(\ell, m) \quad (35)$$

The L fingers of the desired signal are then coherently combined[30] to form the array desired signal output:

$$Y_\kappa^{des}(d_{des}) = \sum_{\ell=1}^{L} \left\{ \left| Z_{za,\kappa}^{des}(n_{\ell=1} T_s) \right| + \ldots + \left| Z_{za,\kappa}^{des}(n_{\ell=L} T_s) \right| \right\} \quad (36)$$

The interference plus noise components $Z_{za,\kappa}^{int}(n_\ell T_s, d_{des})$ at the time of arrival of the fingers are incoherently added together to form the total array interference plus noise output signal:

$$Y_\kappa^{int}(d_{des}) = \sum_{\ell=1}^{L} \left\{ Z_{za,\kappa}^{int}(n_{\ell=1} T_s) + \ldots + Z_{za,\kappa}^{int}(n_{\ell=L} T_s) \right\} \quad (37)$$

2.6.3 Conventional and Distributed Array Combining

The conventional array weight vector in (21) and (34) for each of the three arrays (in the three sectors) in each cell is determined only from the signals lying in the (± 60° relative to the array boresight) sector covered by each array. Combining of the desired signals of the three arrays can be done with either selection combining or maximum ratio combining [8, 9]. In the case of selection combining, the largest desired signal of the three array output signals are selected. In the case of maximum ratio combining, the desired signal components of the three array signals are added coherently for each sample.

The desired signal d is received by all three the distributed arrays in each cell. The beamforming of the three arrays can be done in two ways, 1) independent beamforming or 2) combined beamforming.

The weight vector in (21) and (34) for independent beamforming is determined seperately for each of the three arrays, which will be discussed in more detail in section 2.7. Selection

combining or maximum ratio combining can then be applied to combine the three signals [8, 9]. In the case of selection combining, the largest desired signal of the three array output signals are selected. In the case of maximum ratio combining, the desired signal components of the three array signals are added in phase.

The weight vector in (21) and (34) for combined beamforming is determined for all three sub-arrays together, i.e. the three sub-arrays form one large array. This will be discussed in more detail on section 2.7. The output of all three sub-arrays are then summed to obtain the output of the total combined array optimized for user d_{des} as:

$$Y_{TOT,d_{des}} = \sum_{\kappa=1}^{3} Y_{\kappa,d_{des}} \tag{38}$$

2.7 Weight Vector Estimation

Each of the signals at the antenna elements (after downconversion) is multiplied by a different complex value, or weight. The set of weight values are called a weight vector. The weight vector steer a phased array beam in a specific direction or form a beam matched to the incoming wavefront which maximizes the signal to noise ratio for the adaptive array.

Two different techniques to estimate the weight vector of an adaptive array are discussed in this section. They are the least mean squares method and the direct matrix inversion method. In addition, the required weight vector to steer a phased array in a specific direction is also given.

2.7.1 Adaptive Arrays

The weight vector of an adaptive array is usually determined with optimum combining [2,54,56]. The least mean squares and direct matrix inversion techniques are subsets of optimum combining.

[30] Using a maximum ratio combiner.

2.7.1.1 Optimum Combining

Optimum combining is equivalent to maximum ratio combining (MRC) in the absence of interferers or when both the interferers and noise are white[31] [2]. Optimum combining yields the maximum signal to interference plus noise ratio [54] and is used throughout this thesis. An eigenvalue solution for the weight vector maximizing the SINR is given in [60] and is repeated in Appendix D for completeness. The result is presented in this section. The array output signal is [54]:

$$Y = \mathbf{W}^H \mathbf{X} = \mathbf{W}^H (S_{des}\mathbf{U}_{des} + S_{int}\mathbf{U}_{int} + \mathbf{n}_s) \tag{39}$$

where $\mathbf{U}_{des}$ and $\mathbf{U}_{int}$ are the normalized (with respect to data sequences) desired and interfering signals, S_{des} and S_{int} are the data sequences of the desired and interfering signals and $\mathbf{n}_s$ is the noise vector. The desired signal portion of the output signal is:

$$Y_{des} = \mathbf{W}^H \mathbf{U}_{des} S_{des} \tag{40}$$

and the interference portion of the output signal is:

$$Y_{int+noise} = \mathbf{W}^H (S_{int}\mathbf{U}_{int} + \mathbf{n}_s) \tag{41}$$

Using (40) and (41), the average output signal to interference plus noise power ratio (SINR) is then given by:

$$SINR = E\left\{\frac{|Y_{des}|^2}{|Y_{int+noise}|^2}\right\} = E\left\{\frac{(\mathbf{W}^H S_{des}\mathbf{U}_{des})(S_{des}\mathbf{U}_{des})^H \mathbf{W}}{\mathbf{W}^H (S_{int}\mathbf{U}_{int} + \mathbf{n}_s)(S_{int}\mathbf{U}_{int} + \mathbf{n}_s)^H \mathbf{W}}\right\} \tag{42}$$

which is equal to:

$$SINR = \frac{P_{des}\mathbf{W}^H \mathbf{U}_{des}\mathbf{U}_{des}^H \mathbf{W}}{\mathbf{W}^H (P_{int}\mathbf{U}_{int}\mathbf{U}_{int}^H + \sigma_N^2)\mathbf{W}} \tag{43}$$

where σ_N^2 is the noise power and E{ } is the average taken over several symbols of the baseband data. Assuming without loss of generality that the power of the desired and interference signals is equal to one, (43) can be written as:

[31] Random with a Gaussian distribution.

$$SINR = \Gamma = \frac{\mathbf{W}^H \mathbf{U}_{des} \mathbf{U}_{des}^H \mathbf{W}}{\mathbf{W}^H \mathbf{R}_{nn} \mathbf{W}} \quad (44)$$

where $\mathbf{R}_{nn}$ is the interference plus noise co-variance matrix, equal to [54]:

$$\mathbf{R}_{nn} = \mathbf{U}_{int} \mathbf{U}_{int}^H + \sigma_N^2 \quad (45)$$

The optimum weight vector, $\mathbf{W}_{opt}$, which maximizes the SINR (45) is (see Appendix D and Appendix E):

$$\mathbf{W}_{opt} = \mathbf{R}_{nn}^{-1} \mathbf{U}_{des} \quad (46)$$

2.7.1.1.1 Least Mean Squares

A least mean squares (LMS) algorithm is an iterative solution of the optimum weight vector for an adaptive antenna array. The LMS algorithm minimizes the gradient of the mean square of a cost function, which is the error between a reference signal[32] and the output signal. In the limit, the weight vector will tend towards the optimum weight vector as given in (46). The cost function for the desired user d_{des} is given by the difference between the output of the array and a reference signal [2]:

$$\varepsilon_{d_{des}}(nT_s) = ref^*_{d_{des}}(nT_s) - Y_{TOT,d_{des}}(nT_s) \quad (47)$$

where * denotes the complex conjugate, $ref^*_{d_{des}}$ is a reference signal of mobile d_{des}, n is the optimization iteration number, T_s is sampling period and $Y_{TOT,d_{des}}$ is the total array output (all three sub-arrays) for user d_{des}. The approximate weight vector $\hat{\mathbf{W}}_{\kappa,d_{des}}(nT_s)$ of array κ can be updated using the algorithm, which is [2]:

$$\hat{\mathbf{W}}_{\kappa,d_{des}}[(n+1)T_s)] = \hat{\mathbf{W}}_{\kappa,d_{des}}(nT_s) + \mu \mathbf{X}_{za,\kappa}(nT_s) \varepsilon_{d_{des}}(nT_s) \quad (48)$$

where $\mathbf{X}(nT_s)$ is the array received baseband vector, given in (24) for the narrowband system and (29) for the wideband case. $\hat{\mathbf{W}}_{\kappa,d_{des}}[(n+1)T_s]$ is a new estimate of the weight vector at iteration (n+1), and μ is the convergence constant. The convergence constant is

[32] The reference signal is a sequence correlated with the transmitted desired signal, which is typically known at the receiver.

greater than zero and usually less than one. The speed (or rate) of the LMS convergence is a function of the convergence constant. The larger the constant, the faster the algorithm will converge with a larger variation in the final converged result. A value of 0.08 was used in the simulations in [24]. The elements of the initial weight vector are taken as:

$$\begin{aligned} W_{\kappa,d_{des},m}(0)&=1 \quad \text{for} \quad m=1 \\ W_{\kappa,d_{des},m}(0)&=0 \quad \text{for} \quad m\in[2,3,...,M] \end{aligned} \tag{49}$$

where m is the element number, and M is the number of array elements. This means that for the initial condition, only the first element of each sub-array is receiving. The LMS algorithm will maximize the ratio of the desired signal d_{des} power to the sum of the co-channel interference plus noise signal powers, given by:

$$SINR_{d_{des}}=\frac{Y_{TOT,d_{des}}\,Y^{*}_{TOT,d_{des}}}{\left[\sum_{d=2}^{D} Y_{TOT,d_{des}}\,Y^{*}_{TOT,d_{des}}\right]} \tag{50}$$

where $Y_{TOT,d_{des}}$ is the array output optimized for the desired signal. The maximum ratio of SINR that can be obtained with the LMS algorithm will be constrained by the distance between the mobiles. The iteration process in (48) optimizing the steering vector is continued until a certain acceptable minimum SINR for all the co-channel users is obtained, or until a maximum allowable number of iterations has been reached.

In order to maximize the SINR, a large correlation between the desired signal and the reference signal are required and small correlation between the reference signal and the interference signals. There should also be minimum correlation between the interference signals to obtain the maximum SINR. The training sequence in a GSM system used for channel equalization has this property and has been used as a reference signal in [22]. There are eight training sequences in GSM with a length of 26 bits each. The method described here is able to spatially isolate more than eight users at a time in the same-cell, and therefore the number of sequences in a GSM system is inadequate. Instead, Gold sequences with the same correlation properties as the GSM training sequences, but with a larger number of sequences can also be used [17].

2.7.1.1.2 Direct Matrix Inversion

To evaluate the performance of an adaptive array, the least mean squares estimation method (see section 2.7.1.1.1) can be used to obtain the weight vector. However, this method has a slow convergence. In order to improve the weight convergence time, the direct matrix inversion method was used for most of the simulations in this thesis. The optimum weight vector estimation using the direct matrix inversion method is [51]:

$$\mathbf{W} = \mu \mathbf{R}^{-1} \mathbf{U}_{d_{des}} = \mu_{nn} \mathbf{R}_{nn}^{-1} \mathbf{U}_{d_{des}} \tag{51}$$

where $\mathbf{U}_{d_{des}}$ is the desired signal propagation vector and $\mathbf{R}^{-1}$ is the inverse of the full covariance matrix and μ is a constant given by:

$$\mu = \frac{1}{\mathbf{U}_{des}^{H} \mathbf{R}^{-1} \mathbf{U}_{des}} \tag{52}$$

The desired signal angle of arrival have to be estimated with subspace methods such as MUSIC or ESPRIT. Using the derivation in Appendix E, the optimum weight vector can be written in terms of the inverse of the interference covariance matrix $\mathbf{R}_{nn}^{-1}$ as:

$$\mathbf{W} = \mu_{nn} \mathbf{R}_{nn}^{-1} \mathbf{U}_{d_{des}} \tag{53}$$

where μ_{nn} is also a constant given:

$$\mu_{nn} = \frac{1}{\mathbf{U}_{des}^{H} \mathbf{R}_{nn}^{-1} \mathbf{U}_{des}} \tag{54}$$

It is also shown in Appendix E that the contant μ_{nn} cancels out when estimating the SINR. Assuming that the noise is not correlated with the signals at the antenna elements, the co-variance matrix can be written as [51]:

$$\mathbf{R}_{nn} = E\left\{\mathbf{X}^{int}(nT_s)\left(\mathbf{X}^{int}(nT_s)\right)^{H}\right\} + \sigma_N^2 \mathbf{I} \tag{55}$$

where E{} is the average. If the average in (55) is taken over N samples of the baseband data, the co-variance matrix becomes

$$\mathbf{R}_{nn} = \frac{1}{N} \sum_{n=1}^{N} \mathbf{X}^{int}(nT_s)\left(\mathbf{X}^{int}(nT_s)\right)^{H} + \sigma_N^2 \mathbf{I} \tag{56}$$

where $\mathbf{X}^{int}(nT_s)$ is vector at sample time n, containing the interference (excluding noise) received signals at the array elements after downconversion to baseband (see section 2.6 for more detail about array received signal vector), T_s is the sample period, $\mathbf{I}$ is the unity matrix and σ_N^2 is the noise power. If 1) the average in (56) is much less than the fading rate (or time between fades[33]), the propagation vector (or channel) is assumed to be stationary (or constant) over the period N*Ts and 2) the interfering signals arriving at the array are uncorrelated over the same averaging period (N*Ts), the co-variance matrix can be written as (see Appendix A)

$$\mathbf{R}_{nn} = \sum_{\substack{d=1 \\ d \neq d_{des}}}^{D} P_d \, G_{\kappa,d} \left\{ \mathbf{U}_d(nT_s) \mathbf{U}_d^H(nT_s) \right\} + \sigma_N^2 \mathbf{I} \tag{57}$$

where $\mathbf{U}_d$ is the array vector in the direction of the d^{th} interferer, P_d is the power of the d^{th} interferer and G is the pathloss defined in section 2.4. For independent array beamforming (see section 2.6.3), the weight vector for each sub-array is obtained, or

$$\mathbf{W}_{\kappa,d_{des}} = \mathbf{R}_{nn,k}^{-1} \mathbf{U}_{d_{des},\kappa} \tag{58}$$

where $\mathbf{R}_{nn,\kappa}^{-1}$ is the inverse of the covariance matrix of the independent arrays. Using equation (56) in (58), the weight vector for independent arrays beamforming is:

$$\mathbf{W}_{\kappa,d_{des}} = \left\{ \frac{1}{N} \sum_{n=1}^{N} \mathbf{X}_\kappa(nT_s) \, \mathbf{X}_\kappa^H(nT_s) + \sigma_n^2 \mathbf{I} \right\}^{-1} \mathbf{U}_{d_{des}} \tag{59}$$

For combined array beamforming (see section 2.6.3), $\mathbf{R}_{nn}^{-1}$ and $\mathbf{U}_{d_{des}}$ are the covariance matrix and desired propagation vector of all three combined sub-arrays. Using equations (51) and (56), the combined array weight vector is:

$$\mathbf{W} = \left\{ \frac{1}{N} \sum_{n=1}^{N} \mathbf{X}_{\cap(\kappa)}(nT_s) \, \mathbf{X}_{\cap(\kappa)}^H(nT_s) + \sigma_n^2 \mathbf{I} \right\}^{-1} \mathbf{U}_{d_{des},\cap(\kappa)} \tag{60}$$

[33] This is the channel coherence time or time that the channel remains constant. This time is the speed of the mobile divided by the wavelength.

where $\mathbf{X}_{\cap(\kappa)}$ is the concatenated vector of the 3 distributed sub-array receive signal vectors and $\mathbf{U}_{desired,\cap(\kappa)}$ is the concatenated vector of the 3 distributed sub-array desired signal steering vectors

2.7.1.1.3 Simultaneous Co-channel Weight Estimation

In the case of a reuse factor of one (see section 2.2.2) and multiple users operating on the same channel (for TDMA and GSM type systems) in the same cell, the users can be isolated[34] from each other with adaptive beamforming. This is done by creating spatial channels between the users, called space division multiple access or SDMA [22]. In the case where there are D co-channel users in the same cell, the number of co-channel interferers is D-1 for every desired user. An adaptive beam is formed for each user from the sampled and downconverted signals at the antenna elements. The adaptive beam is formed by determining an optimum set of weights for each user. There are thus D sets of weights, with the length of each set equal to the number of elements per array multiplied by the number of arrays, as shown in Figure 21.

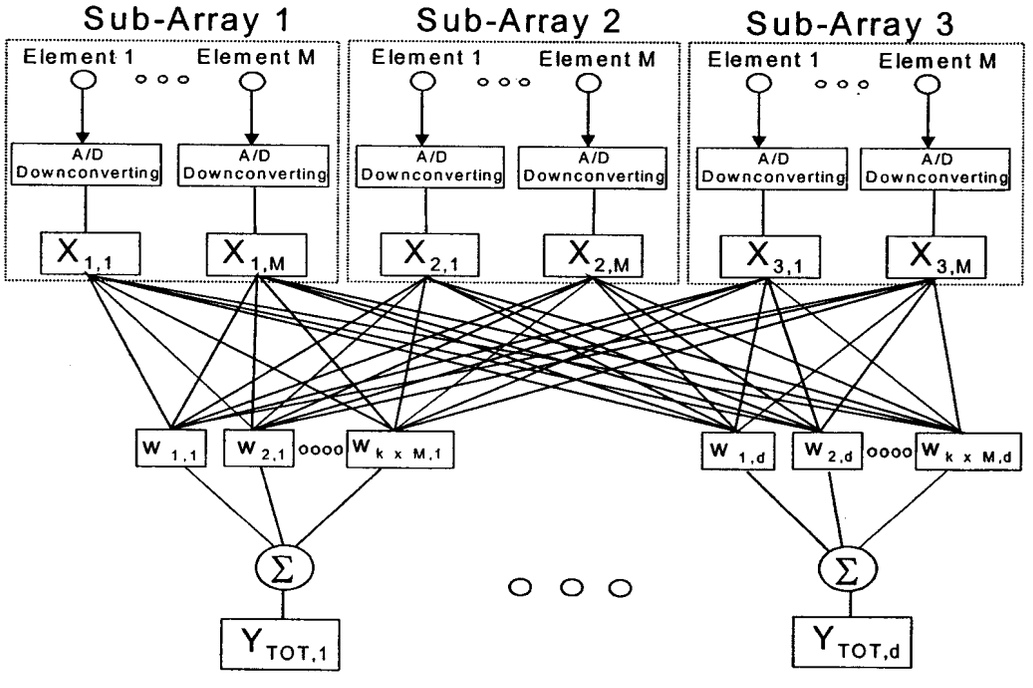

Figure 21: Simultaneous co-channel up-link adaptive beamforming estimation diagram.

[34] In order to extract the data transmitted by each user.

2.7.2 Phased Arrays

A phased array steers a beam in the direction of the desired signal by generating a linear phase across all the array elements [51]. The phased array weight **W** for the desired signal d_{des} is given by:

$$\mathbf{W}_{\kappa,d_{des}} = \mathbf{U}_{d_{des}}(\psi^{c}_{z,za,\kappa,d_{des}}) \tag{61}$$

where $\psi^{c}_{z,za,\kappa,d_{des}}$ is the angle towards the desired mobile in cell z and boresight angle of sub-array κ in cell za and $\mathbf{U}_{d_{des}}$ is the array propagation vector of the desired mobile.

2.8 Distribution of mobiles

In this thesis it is assumed that mobile positions are distributed uniform with respect to area. The histogram for a hexagonal cell structure of the mobile to BTS radius is shown in Figure 22. The figure shows that the probability increases linearly with radius up to 0.866 times the radius, after which it decreases non-linear with radius up to the cell radius (cell radius is 1000m in the figure).

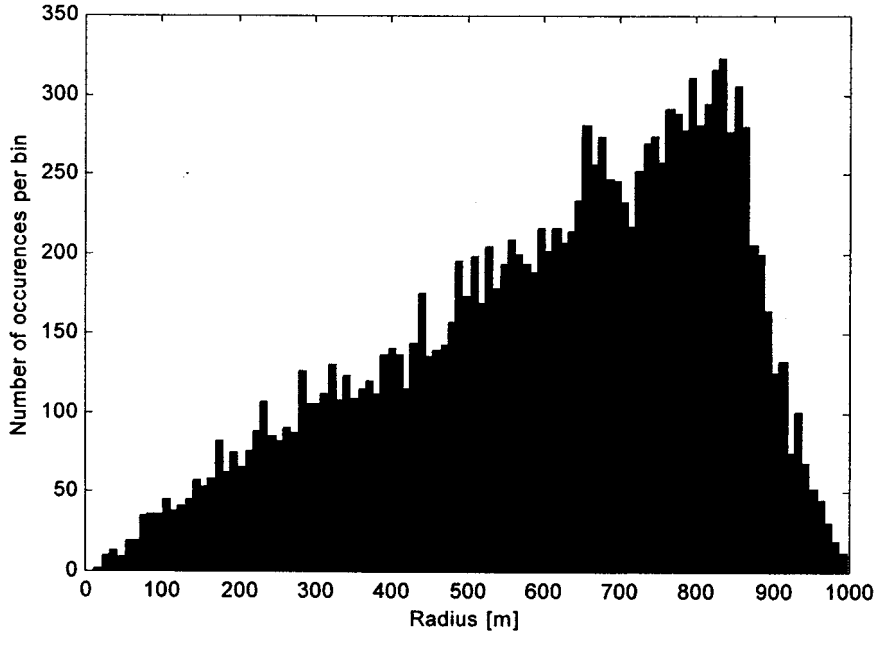

Figure 22: Histogram of mobile to BTS radius with a cell radius of 1000m.

2.9 Performance Evaluation

2.9.1 Monte-Carlo Simulations

Closed form solutions are difficult to obtain when the signals at the array elements are correlated [11]. Since the aim of this thesis is to investigate the performance of the combined array with closely spaced elements in a narrow angular spread propagation environment, the signals between the array elements are correlated. Closed form solutions are therefore difficult to derive [11]. In order to estimate the performance of these arrays, a Monte-Carlo simulation method will be used in this thesis.

The Monte-Carlo method is a statistical technique. If the system under consideration has a random behavior, a Monte-Carlo simulation will produce an approximation of the distribution (probability density function or cumulative distribution function) of the random process. The signal from a mobile will be scattered by a number of obstacles surrounding the mobile.

The scattered signal reaching the base station will have Rayleigh and Log-normal fading. These fading processes are random processes and therefore ideal candidates for the Monte-Carlo method. In the case of closed form solutions, a number of approximations have to be made in order to find the solution. Depending on the specific problem, Monte-Carlo simulations (apart from simulation time constraints) do not have these closed form constraints (or fewer constraints).

2.9.2 Bit Error Rate

It is assumed in this thesis that the signal is phase-shift keyed modulated. If both the noise and received complex interference signals have a Gaussian distribution, the average bit error rate (BER) for coherent detection of phase-shifted PSK signals is given by [11]

$$BER_{average} = \frac{1}{2}\int_{-\infty}^{\infty} p(\eta)\ \mathrm{erfc}(\sqrt{\eta})\,d\eta \qquad (62)$$

where η is the instantaneous signal to interference plus noise ratio (SINR), p( ) is the probablity density function and erfc is the complimentary error function. In this case the

probability density function can be determined with a Monte-Carlo method. Instead of first determining the PDF, the average bit error rate can be determined directly with a Monte-Carlo method (see section 2.9.1). In this case, the BER for each Monte-Carlo sample (i) is given by:

$$\mathrm{BER}(i) = \frac{1}{2}\mathrm{erfc}\{\mathrm{SINR}(i)\} \tag{63}$$

where SINR(i) is the signal to interference plus noise ratio for sample i. The average BER is then the average of all the Monte-Carlo samples.

2.10 Conclusions

In this chapter the reuse distance of a cellular network was described as well as the effect of sectorization and beamforming on the reuse distance. Different array beamforming techniques, geometries and element patterns were discussed. A detailed formulation of the propagation channel models that will be used in this thesis were presented, including fast and slow fading models. The spatially distributed array concept was introduced and practical implementation issues were discussed. This was followed by a detailed definition of the received signals at the distributed sub-array elements. Methods of combining the sub-array output signals for both narrow and wideband systems were discribed. Estimation techniques of the weight vector for phased and adaptive arrays were discussed, followed by a description of the mobile distributions as well as statistical methods that will be used in the simulations.